Batteries & Supercaps

Research Article
doi.org/10.1002/batt.202400777

Chemistry Europe
European Chemical Societies Publishing

www.batteries-supercaps.org

Multichannel Electrochemical Cell and Liquid-Handling Dispenser for High-Throughput Combinatorial Screening of Multicomponent Electrolytes for Advanced Lithium-Ion Batteries

Shoichi Matsuda* and Misato Takahashi

The performance requirements of Li-ion batteries as energy storage devices are continuously increasing. To meet these demands, optimizing the electrolyte composition, especially for expanding the operating temperature range of LiBs, remains a critical challenge. High-throughput experimentation represents an effective approach for accelerating the discovery of multicomponent electrolytes. However, most high-throughput experiment studies on battery electrolytes are focused on evaluating the battery performance at room temperature owing to the challenges of integrating temperature control systems. To address this limitation, this study introduces a high-throughput experimental setup composed of a (i) closed-type 36-well multichannel electrochemical cell module, (ii) noncontact liquid-handling dispenser, and (iii) multielectrochemical analyzer installed within a temperature-controlled chamber. This setup enables the preparation of multicomponent electrolyte additives in a combinatorial manner and the evaluation of battery performance with the prepared electrolytes across a wide temperature range, achieving a throughput of over 400 samples per week.

1. Introduction

The demand for enhancing the performance of Li-ion batteries (LiBs) as energy storage devices is growing. In particular, enhancements such as increased cell-level energy density, prolonged cycle life, reduced charging time, and extended operating temperature range are highly desirable for the industrial application of LiBs. To meet these requirements, advanced electrolyte materials must be identified. Electrolytes not only facilitate Li-ion transport between the negative and positive electrodes but also contribute to the formation of a stable electrode–electrolyte interface, which considerably affects the overall performance of LiBs.[1,2] For instance, at the graphite negative electrode, the reductive decomposition of electrolyte components results in the formation of a solid–electrolyte interphase (SEI). Ideally, the SEI must be electronically insulating yet Li-ion conductive, preventing further electrolyte decomposition while enabling the reversible intercalation and deintercalation of Li ions into the graphite electrode. In general, to optimize SEI formation, various compounds are incorporated into electrolytes as additives. As these additives work synergistically to facilitate SEI formation, the appropriate combinations that can promote the formation of an ideal SEI must be identified to maximize LiB performance. However, predicting the optimal combination remains challenging owing to the complexity of the SEI formation process. Despite extensive experimental and computational efforts, the precise formation mechanism and structure of the SEI remain elusive. Thus, researchers often rely on conventional trial-and-error methods to identify the optimal additive combinations, which are time- and cost-intensive.

High-throughput experimental techniques offer a promising approach for accelerating electrolyte development.[3–7] Previously, we developed a 96-well microplate-based multichannel electrochemical (MCE) cell system and used it to conduct automated experiments for screening multicomponent electrolyte additives for LiBs, achieving a throughput of over 1000 samples per day.[8–10] This system, installed in an argon-filled glove box, consisted of a liquid-handling dispenser, multielectrochemical analyzer, plate stacker, and robotic arm. Using a data-driven search algorithm, we identified a combination of five chemicals that enhanced battery cycle life. Although this system proved effective for electrolyte additive screening, several technical challenges remain for further methodological improvements.

One challenge is electrolyte volatilization. As the microplate-based electrochemical cell is not completely sealed,

S. Matsuda, M. Takahashi
Center for Green Research on Energy and Environmental Materials
National Institute for Material Science
1-1 Namiki, Tsukuba, Ibaraki 305-0044, Japan
E-mail: MATSUDA.Shoichi@nims.go.jp

S. Matsuda
Center for Advanced Battery Collaboration
National Institute for Material Science
1-1 Namiki, Tsukuba, Ibaraki 305-0044, Japan

S. Matsuda
NIMS-SoftBank Advanced Technologies Development Center
National Institute for Material Science
1-1 Namiki, Tsukuba, Ibaraki 305-0044, Japan

Supporting information for this article is available on the WWW under https://doi.org/10.1002/batt.202400777

Research Article
doi.org/10.1002/batt.202400777
Chemistry Europe
European Chemical Societies Publishing

high-vapor-pressure components gradually evaporate, leading to electrolyte depletion. Another challenge is temperature control. From a practical standpoint, evaluating battery performance across a wide temperature range is desirable.[11–13] However, precise temperature control within the Ar-filled glove box during battery cycling is difficult owing to space constraints.

To address these limitations, in this study, we establish a high-throughput experimental setup consisting of a (i) closed-type 36-well MCE cell module, (ii) a noncontact liquid-handling dispenser, and (iii) multielectrochemical analyzer housed within a temperature-controlled chamber (**Figure 1**). The noncontact liquid-handling dispenser enables rapid electrolyte mixing and injection into the MCE cell module, within a few minutes (36 wells). Additionally, each MCE cell is tightly sealed with bolted caps to minimize electrolyte volatilization. Thus, this system allows the preparation of multicomponent electrolyte additives in a combinatorial manner and enables battery performance evaluation across a wide temperature range, achieving a throughput of over 400 samples per week. Notably, this setup eliminates the need for a robotic arm for MCE cell transport, further streamlining the workflow. The proposed methodology offers an effective means for accelerating the discovery of multicomponent electrolytes for advanced LiBs.

2. Results and Discussion

Automated robotic experimental techniques represent an effective approach for preparing a wide range of electrolyte solutions with diverse compositions. Various automated liquid-handling systems are commercially available at present. Using these technically established devices appropriately, the electrolyte-preparation process can be automated with high throughput. In standard laboratory procedures, electrolyte preparation typically involves three key steps: (i) weigh solid compounds, (ii) add liquid compounds in appropriate volumes, and (iii) stir the solution to ensure complete dissolution of solid compounds. Automated robotic systems are typically designed to perform specific tasks with high accuracy and throughput. Therefore, to realize the standard electrolyte-preparation process using automated robotic systems, at least three types of robotic equipment must be available: (i) for weighing solid compounds, (ii) for injecting liquid compounds, and (iii) for stirring solutions. However, the introduction of multiple automated robotic systems necessitates significant cost and space. These requirements hinder the implementation of automated robotic systems in laboratory settings.

Considering these aspects, this study focuses on an alternative approach to electrolyte preparation, in which several types of solutions, with solid compounds pre-dissolved, are mixed. Thus, electrolyte solutions with different compositions can be effectively prepared by appropriately selecting the solutions and controlling the mixing ratio. Importantly, this method requires only a single automated robotic system (liquid-handling dispenser) for electrolyte mixing, which helps minimize investment cost and space requirements. In this study, the noncontact liquid dispenser, CERTUS, is selected, which can mix up to eight different solutions with accuracy at the nanoliter scale (Figure S1, Supporting Information). Using this dispenser, multicomponent electrolytes with various compositions can be prepared in a combinatorial manner within minutes.

When preparing electrolytes by mixing several solutions, the expression of the electrolyte composition must be carefully treated. For example, consider a multicomponent electrolyte composed of $LiPF_6$, $LiBF_4$, lithium difluoro(oxalato)borate (LiBOB), ethylene carbonate (EC), propylene carbonate (PC), vinylene carbonate (VC), and fluoroethylene carbonate (FEC), which are commonly used for preparing LiB electrolyte solutions. In general, the composition of electrolyte solutions is expressed in terms of molar concentration (mol/L), while the composition of additives is expressed in terms of weight percentage (wt%). For instance, the representative expression for a LiB electrolyte LiB is 0.5 M $LiPF_6$ + 0.5 M $LiBF_4$ in EC/PC (30:70 vol%) with 1 wt% LiBOB, 5 wt% VC, and 5 wt% FEC. However, this expression presents several problems in the case of multicomponent electrolytes. First, the Li salt concentration is indicated in units of mol L^{-1}. The denominator of this unit represents the volume of the entire solution,

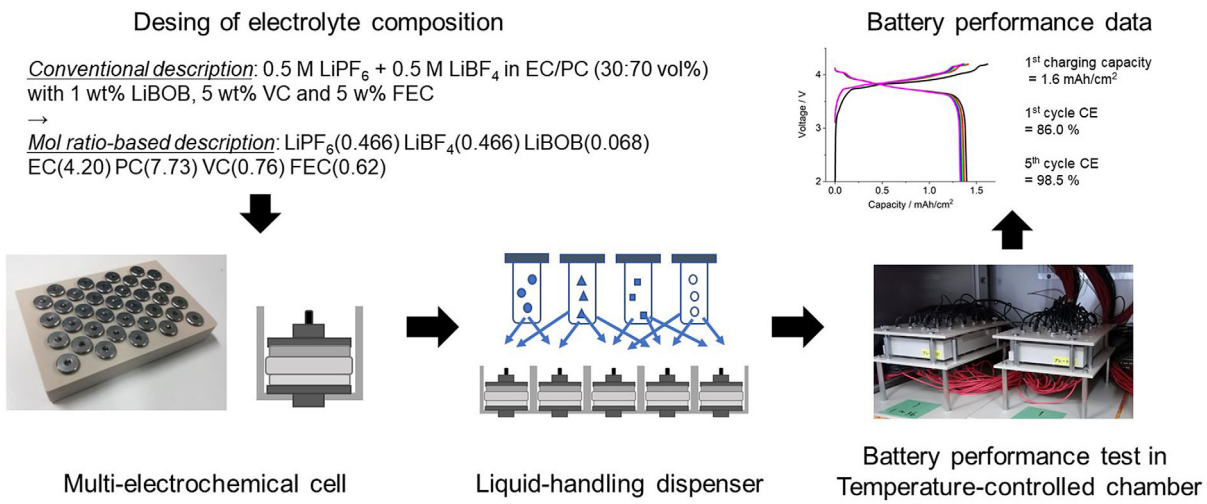

Figure 1. Schematic of proposed approach for high-throughput combinatorial screening of multicomponent electrolytes for advanced lithium-ion batteries.

which may change owing to solvent mixing and dissolution of Li salt. In the case of a multicomponent electrolyte, the dissolution of a large amount of Li salt may alter the solution volume, and this change may be challenging to accurately predict. Consequently, when using the mol L^{-1} unit, the final volume of the electrolyte solution must be measured. Second, additive concentrations are typically expressed in wt%. When the additive content exceeds 10 wt%, the concentration of the principal components may diminish by ≈10%. Consequently, expressing electrolyte composition based on the weight percentage may not be an accurate representation.

One effective approach for addressing the aforementioned problem is to express all chemical compositions in terms of their molar ratios. For example, the electrolyte composition can be expressed as $LiPF_6$ (0.466) $LiBF_4$ (0.466) LiBOB (0.068) EC (4.20) PC (7.73) VC (0.76) FEC (0.62). By defining the following six parameters, the electrolyte can be defined in a manner that represents its physicochemical properties, such as concentration and solvent ratio.

$$x = \frac{LiPF_6}{LiPF_6 + LiBF_4 + LiBOB} \tag{1}$$

$$y = \frac{EC + PC + VC + FEC}{LiPF_6 + LiBF_4 + LiBOB} \tag{2}$$

$$z = \frac{EC}{EC + PC + VC + FEC} \tag{3}$$

$$a = \frac{LiBOB}{LiPF_6 + LiBF_4 + LiBOB} \tag{4}$$

$$b = \frac{VC}{EC + PC + VC + FEC} \tag{5}$$

$$c = \frac{FEC}{EC + PC + VC + FEC} \tag{6}$$

In these expressions, x and a represent the ratios of $LiPF_6$ and LiBOB among the Li salts, respectively; and z, b, and c represent the EC, VC, or FEC ratios among the solvents. The electrolyte composition can be consistently expressed using these six parameters, as the electrolyte is composed of six chemical compounds. Furthermore, the constituents of the electrolyte can be expressed in terms of the molar ratio using the aforementioned parameters through mutual conversion.

$$LiPF_6 = x \tag{7}$$

$$LiBOB = a \tag{8}$$

$$LiBF_4 = 1 - (x + a) \tag{9}$$

$$EC = yz \tag{10}$$

$$VC = yb \tag{11}$$

$$FEC = yc \tag{12}$$

$$PC = y * (1 - (z + b + c)) \tag{13}$$

Consider the actual preparation of electrolytes using the liquid-handling dispenser. As the design principle for the mother solution, first, solutions with a high concentration level of Li salts must be prepared, as they can be subsequently diluted with solvents to achieve electrolytes with lower Li salt concentration. In the case of the sample electrolyte, EC and PC are the main solvents, while $LiPF_6$ and $LiBF_4$ are the main Li salts. Thus, the following four mother solutions should be prepared:

1: EC solution with a high concentration of $LiPF_6$.
2: PC solution with a high concentration of $LiPF_6$.
3: EC solution with a high concentration of $LiBF_4$.
4: PC solution with a high concentration of $LiBF_4$.

In addition, a solution with a high concentration of LiBOB should be prepared, along with a pure PC solvent.

5: PC solution with a high concentration of LiBOB.
6: Pure PC solvent.

Notably, an EC-based solution with LiBOB or pure EC solvent is not included as a mother solution owing to the limited solubility of LiBOB into EC and the fact that EC is a solid at room temperature. Lastly, pure VC and FEC solvents are selected as mother solutions.

7: Pure VC solvent.
8: Pure FEC solvent.

The compositions of these eight mother solutions are summarized in Table S1, Supporting Information.

To conduct electrolyte-preparation experiments using a liquid-handling dispenser, it is necessary to consider the number of electrolyte solutions that can be prepared by mixing the eight mother solutions. Figure S2, Supporting Information, illustrates the mother solution mixing protocol. First, the required amount of $LiPF_6$ or EC is introduced by injecting mother solution No. 1. In the case of 54 candidates, the required amount of EC can be supplied using only mother solution No. 1. For these candidates, the next step is to add the required amount of $LiPF_6$ using mother solution No. 2 ($LiPF_6$ (1) PC (10)). For the other 189 candidates, the remaining amount of EC against the required level is introduced using mother solution No. 3 ($LiBF_4$ (1) EC (7.5)). The required amount of LiPF6 or EC for all 234 candidates is introduced by adding appropriate quantities of mother solutions. The next step involves the addition of mother solutions No. 4 ($LiBF_4$ (1) PC (4)) and No. 5 (LiBOB (1) PC (200)) to meet the required amounts of $LiBF_4$ and LiBOB, respectively. However, for 44 candidates, the amount of PC exceeds the required level upon adding these solutions. For the remaining 199 candidates, the required amounts of VC and FEC are introduced by adding mother solutions No. 7 and No. 8. As shown in Figure S2, Supporting Information, 236 candidate electrolytes can be prepared by mixing eight mother solutions in the appropriate ratios.

This procedure enables the realization of various electrolyte compositions using a liquid-handling dispenser by simply mixing several mother solutions in the appropriate ratio. Furthermore, electrolyte mixing and injection into the MCE cell module can be accomplished in a single step, thereby, improving the total throughput of the experiments. Although a specific liquid-handling dispenser is used as the model equipment in this study,

Research Article
doi.org/10.1002/batt.202400777
Chemistry Europe
European Chemical Societies Publishing

the proposed methodology can be applied to other liquid-handling dispensers. One MCE cell module contains 36 independent electrochemical cells, arranged to be compatible with the automatic dispensing equipment. Each electrochemical cell can be assembled with a positive electrode, separator, and negative electrode using a semiautomated punching equipment (Figure S3, Supporting Information), and the electrolyte can be injected directly from the liquid-handling dispenser. Following electrolyte injection, electric connection parts are installed within each MCE cell (Figure S4, Supporting Information). Subsequently, the MCE cells are tightly sealed by capping their tops with bolts, thereby, suppressing electrolyte volatilization (Figure S5, Supporting Information). The prepared MCE cell is then electrochemically connected to a suitable multichannel battery tester, allowing for parallel assessment of the battery performance of different cells (Figure S6, Supporting Information). Details of the experimental procedure for MCE cells are provided in Figure S7, Supporting Information.

Figure 2a shows the representative charge/discharge profiles obtained from an MCE cell. These experiments involved a graphite negative electrode (5 mg cm^{-2}, 1.6 mAh cm^{-2}), a $LiCoO_2$ positive electrode (10 mg cm^{-2}, 1.5 mAh cm^{-2}), and an electrolyte solution of 1 M $LiPF_6$ in EC:PC (1:1 vol%). To mitigate concerns regarding electrolyte wettability on the separator, a glass fiber separator was used. The results demonstrate that stable charge/discharge reactions proceeded in all cells with a current density of 0.1 mA cm^{-2}. At 25°C condition, the 1st charging capacity exhibited ≈1.5 mAh cm^{-2}. In contrast, in 1st discharge process, capacity is 1.0 mAh cm^{-2}. Such low capacity in the 1st discharge process is due to the large irreversible capacity caused by SEI formation process because the electrolyte does not contain suitable SEI forming additives to minimize the irreversible capacity during 1st cycle. Finally, the coulombic efficiency (CE) of the 5th cycle was 97.9%. After the measurement, the temperature was increased to 60°C and an additional five-cycle test was performed. In this condition, the capacity gradually decreased with cycling. Thus, the CE of the 5th cycle was 91.6% (Figure 2b). The experiments were repeated using three different cells, and the standard deviation was recorded. The standard deviation of the 5th CE was 0.17% at 25 °C and 0.61% at 60 °C, revealing the high reproducibility in battery performance testing (Figure 2c).

Next, we discuss the actual experimental throughput of the proposed system for preparing multicomponent electrolytes and assessing their battery performance. This setup involved six MCE cell modules. Using a liquid-handling dispenser, 216 electrolytes were prepared and injected into the MCE cells (36 cells per module × 6 modules = 216 cells). This process could be completed within several hours. Subsequently, the prepared MCE cell modules were subjected to battery performance evaluations in a temperature-controlled chamber. This process required one or

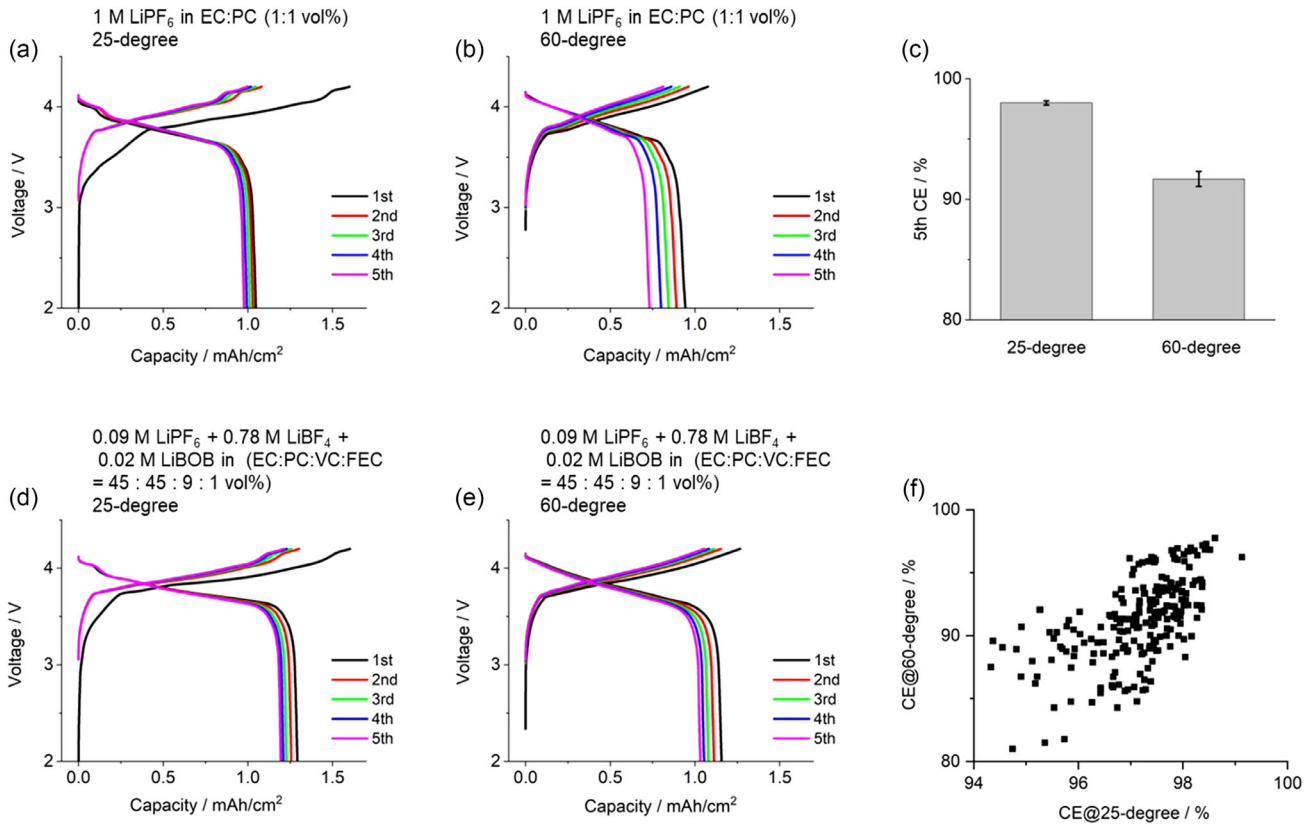

Figure 2. a,b) Charge/discharge profiles obtained using an MCE cell with a graphite negative electrode, a $LiCoO_2$ positive electrode, and an electrolyte of 1 M $LiPF_6$ in EC:PC (1:1 vol%) at a) 25 °C and b) 60 °C. c) 5th CE obtained in each temperature condition. d,e) Charge/discharge profiles of cell with electrolyte composition of 0.09 M $LiPF_6$ + 0.78 M $LiBF_4$ + 0.02 M LiBOB in (EC:PC:VC:FEC = 45:45:9:1 vol%), obtained at d) 25 °C and e) 60 °C. f) Relationship between 5th CE obtained under 25 and 60 °C conditions.

two days. Thus, experiments involving two series of six MCE cell modules could be completed within one week, achieving an experimental throughput of over 400 samples per week.

To demonstrate the effectiveness of the proposed system, we evaluated the battery performance of a multicomponent electrolyte solution consisting of $LiPF_6$, $LiBF_4$, LiBOB, EC, PC, VC, and FEC. We defined 243 potential electrolyte solutions by setting five parameters with three levels each. Thus, the parameter values were set as follows: $x = 0.1$, 0.3, 0.5; $y = 15$; $z = 0.1$, 0.3, 0.5; $a = 0.005$, 0.01, 0.02; b = 0.01, 0.05, 0.1; and c = 0.01, 0.05, 0.1 (Table S2, Supporting Information). Note that these parameters were selected as an example to demonstrate the effectiveness of the experimental setup using MCE cells and a liquid-handling dispenser, and other parameter values could also be selected. Among the 243 candidates, 236 samples could be prepared by mixing the eight mother solutions. The battery performance tests were conducted using $LiCoO_2$ as the positive electrode and graphite as the negative electrode. Repeated charge/discharge tests were performed for five cycles at 25 °C and five cycles at 60 °C with a cutoff voltage of 4.2/2.0 V.

Figure 2f presents the results of the 5th CE of MCE cells containing 236 electrolytes, obtained at 60 °C. Each plot represents data from a single MCE cell with a specific electrolyte composition. At 25 °C, most cells exhibited a 5th CE exceeding 90%. In contrast, at 60 °C, the 5th CE of several cells was below 90%. Research has shown that during charge/discharge cycling at elevated temperatures, the SEI on graphite becomes unstable, leading to the decomposition of electrolyte components. In most of the electrolyte compositions investigated in this study, this side reaction occurred at 60 °C. Consequently, the 5th CE was lower than that at 25 °C. The electrolyte compositions exhibiting the highest 5th CE at 60 °C are listed in Table S3, Supporting Information. Notably, in all top-30 samples, the value of parameter *a* was 0.02, corresponding to the highest concentration of LiBOB. No clear trend was observed for the other parameters (parameter *y* was fixed in this experiment). These results clearly indicate that LiBOB plays a pivotal role in achieving a high 5th CE at 60 °C.

Among the 236 candidates, electrolyte No. 79 (x, y, z, a, b, c) = (0.1, 15, 0.5, 0.02, 0.1, 0.01) exhibited the highest 5th CE at 60 °C. This electrolyte, with a composition of 0.09 M $LiPF_6$ + 0.78 M $LiBF_4$ + 0.02 M LiBOB in (EC:PC:VC:FEC = 45:45:9:1 vol%), achieved a 5th CE of 97.8% at 60 °C. The charge/discharge profiles at 25 and 60 °C are shown in Figure 2d and e, respectively. This composition was characterized by the lowest concentrations of $LiPF_6$ and FEC and the highest concentrations of $LiBF_4$, LiBOB, EC, and VC. LiBOB, EC, VC, and FEC are well-known compounds that act as SEI-forming agents for graphite electrodes.[14–16] In addition, $LiBF_4$ demonstrates greater stability at higher temperatures compared with $LiPF_6$.[17] Therefore, it is reasonable to conclude that an increase in the concentration of these elements results in a higher 5th CE, even at 60 °C.

Table S4, Supporting Information, summarizes the battery performance results for the cell containing electrolytes similar to No. 79. The results indicate that varying *x* and *z* had minimal impact on the battery performance. In contrast, the 5th CE significantly decreased when *a*, *b*, and *c* were varied. Therefore, we focused on the concentration dependence of VC and FEC. Additional experiments were conducted using three different cells, and the standard deviation was assessed. **Figure 3**a shows the 1st CE at 25 °C for five electrolytes with different VC and FEC concentrations. The electrolyte composition (VC: 0.1, FEC 0.01) exhibited the highest 5th CE at 60 °C. These results indicate that increasing VC and FEC concentrations enhanced the 1st CE. Figure S8, Supporting Information, shows the voltage profiles of cells with electrolytes containing different VC and FEC concentrations. The shift in the profile at the beginning of the charging process reveals that the increase in VC and FEC concentrations resulted in a decrease in charge capacity required for SEI formation on the graphite electrode. This result is consistent with the observed increase in the 1st CE at this condition. Figure 3b shows the 5th CE values at 60 °C. Although the increase in VC concentration resulted in enhanced CE, the increase in FEC concentration significantly reduced the 5th CE. These results clearly demonstrate that the increase in VC concentration and decrease in FEC concentration are crucial for maximizing the 5th CE at 60 °C. One possible explanation is that the negative effect of FEC on the positive electrode side is more pronounced at 60 °C. We are currently exploring this phenomenon in greater detail.

Next, we compared the electrochemical evaluation results of our developed MCE cell and a standard coin-type cell. Two electrolytes were considered: 1 M $LiPF_6$ in EC/PC (1:1 vol%) and 0.09 M $LiPF_6$ + 0.78 M $LiBF_4$ + 0.02 M LiBOB in (EC:PC:VC:FEC = 45:45:9:1 vol%). Three independent cells were fabricated for each type of cell, and their battery performance was evaluated

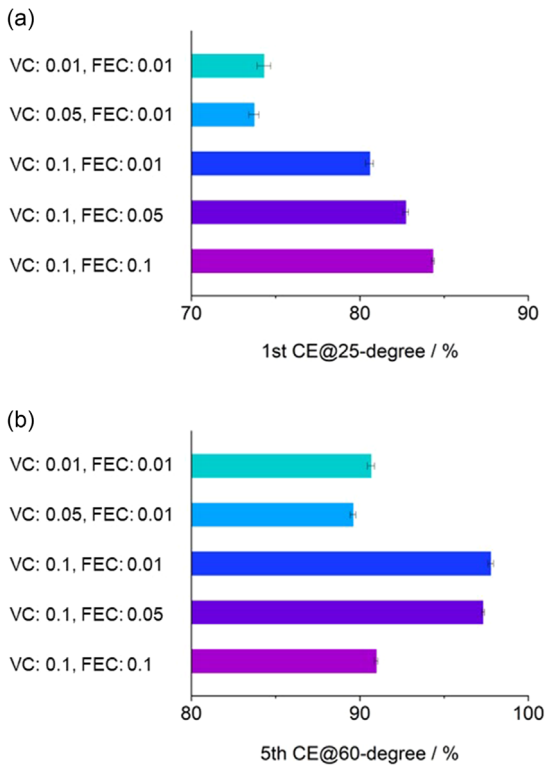

Figure 3. a) Summary of 1st CE at 25 °C condition and b) 5th CE at 60 °C condition, obtained by MCE cell with the electrolyte containing different VC and FEC concentrations level.

Research Article
doi.org/10.1002/batt.202400777
Chemistry Europe
European Chemical Societies Publishing

at 25 and 60°C. At 25°C, both cells exhibited similar profiles, although the 1st CE of the MCE cell was lower than that of the coin-type cell (**Figure 4**a,c). After the five-cycle test at 25°C, the cells were subjected to cycling tests at 60 °C for five additional cycles. The results are summarized in Figure 4b–d, with magnified images shown in Figure S9, Supporting Information. At 60 °C, the CE between the 2nd and 5th cycles exceeded 95% for both electrolytes in the coin-type cell. However, for the MCE cell, the corresponding CE was below 95%. In the coin-type cell, the areal size of the electrode was 2.0 cm^2 and electrolyte amount was 100 μL. Thus, the electrolyte amount per electrode was 50 μL cm^{-2}. In contrast, for MCE cells (areal size of electrode: 0.237 cm^2 and electrolyte amount: 40 μL), this value increased to 168 μL cm^{-2}. The excess electrolyte in MCE cells likely resulted in prominent side reactions, such as electrolyte volatilization and decomposition at the surface of electric connection parts. These differences, related to the miniaturization of electrochemical cells, can likely explain the absolute CE variations observed between the MCE and coin-type cells. Our future work will be aimed at enhancing the design of MCE cells, for example, by minimizing the dead volume.

In this study, battery performance evaluations were primarily conducted at 60 °C. Therefore, we focused on electrolyte systems composed of high-boiling-point solvents, such as PC and EC. Nevertheless, the proposed high-throughput experimental methodology is highly versatile and can also be applied to electrolyte systems containing low-boiling-point solvents, such as dimethyl carbonate and diethyl carbonate. In fact, we are actively applying this methodology for the development of electrolyte materials for next-generation rechargeable battery systems.

Lastly, we examined the experimental throughputs of MCE cells and coin-type cells for electrolyte screening (Figure S10, Supporting Information). Assume that a single technical assistant works for one week, and the maximum number of available battery evaluation channels is 200. In the coin-type cell experiment, the electrolyte is prepared manually. As the electrolyte must be prepared in an Ar-filled glove box, at most 40 electrolyte solutions can be prepared each day. Subsequently, 40 coin-type cells are fabricated, which takes one additional day. By repeating this process two times, it is possible to evaluate the battery performance of 80 electrolyte compositions in one week. In comparison, in the case of MCE cells, more than 200 electrolytes with different compositions can be prepared within one day using a high-speed liquid-handling dispenser. The technical assistant is required to prepare only the mother solution and configure the program for the liquid-handling dispenser. Electrolyte mixing and injection into MCE cells can be simultaneously performed by the liquid-handling dispenser within minutes in a high-throughput manner. The corresponding MCE cells can be fabricated within a single day. By repeating this procedure twice, the battery performance of more than 400 electrolytes can be accomplished within one week.

In this study, the battery performance evaluation was limited to the first five cycles. However, longer cycling tests are required

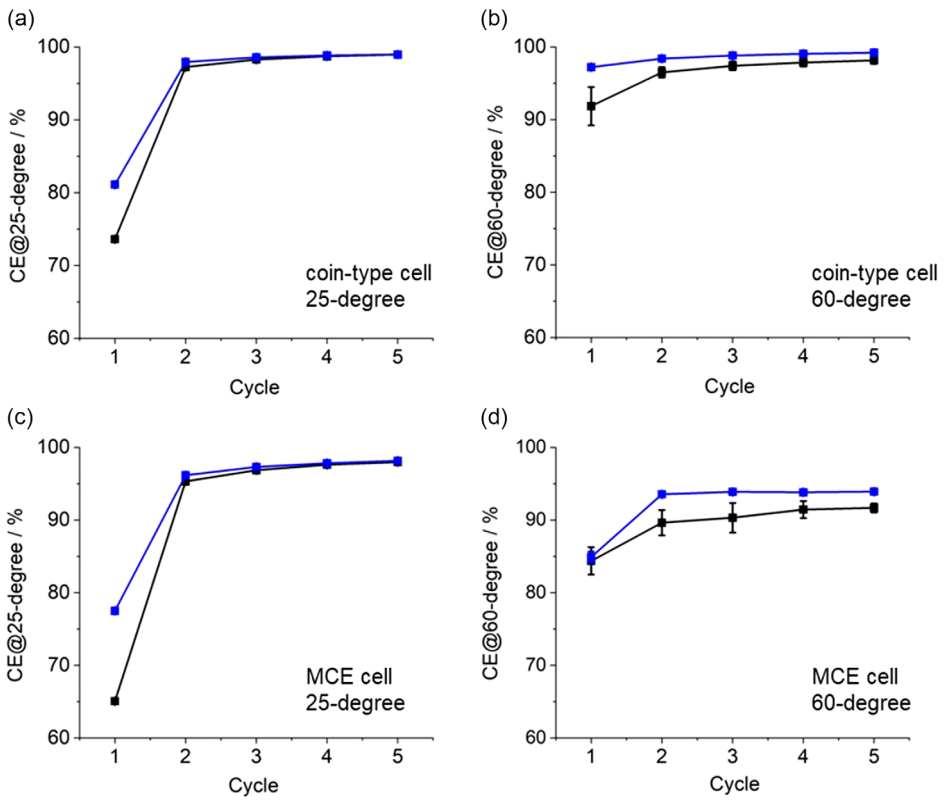

Figure 4. Battery performance evaluation for coin-type cell and MCE cell with electrolytes 1 M $LiPF_6$ in EC:PC (1:1 vol%) (black curve) and 0.09 M $LiPF_6$ + 0.78 M $LiBF_4$ + 0.02 M LiBOB in (EC:PC:VC:FEC = 45:45:9:1 vol%) (blue curve). CE evaluation in a,b) coin-type cell and c,d) MCE cell at a,c) 25 °C and b,d) 60 °C.

to gain deeper insights about the battery performance. Strategies, such as accelerated evaluation protocols or lifetime prediction models, can be adopted to maintain high throughput while ensuring meaningful performance differentiation. Moreover, further advancements in electrolyte material screening methods are necessary, leveraging the advantages of the liquid-handling dispenser, which enables the rapid and precise preparation of a wide variety of electrolytes. Overall, the proposed methodology can accelerate the development of multicomponent electrolytes for maximizing battery performance and help clarify the complex reaction mechanism in LiBs.

3. Conclusion

MCE cells, which are highly compatible with liquid-handling dispensers, were used to construct an electrolyte screening system for LiBs, achieving a high throughput of over 400 samples per week. This system enables the combinatorial preparation of different electrolytes and their direct injection into MCE cells. Battery performance testing can then be performed in temperature-controlled conditions. To demonstrate the effectiveness of the proposed system for identifying multicomponent electrolytes that can enhance LiB performance, we selected a model electrolyte system composed of $LiPF_6$, $LiBF_4$, LiBOB, EC, PC, VC, and FEC and investigated the $LiCoO_2$/graphite battery performance at 60 °C. We experimentally verified the electrolyte composition that exhibited the highest 5th CE among 236 candidates. The systematic investigation also revealed that a high concentration of LiBOB is crucial for achieving a high 5th CE at this temperature. This study offers a high-throughput experimentation system for accelerating the discovery of multicomponent electrolytes to enhance the performance of next-generation rechargeable batteries. In particular, by combining autonomous search algorithms,[10] the efficiency of complex optimization processes, conventionally performed through time- and labor-intensive trial-and-error based approaches, can be enhanced.

Acknowledgements

The authors thank Dr. Yuki Maruyama for providing technical assistance in the experiments. This work was partially supported by JST COI-NEXT (grant no. JPMJPF2016) and Ministry of Education, Culture, Sports, Science, and Technology (MEXT) Program: Data Creation and Utilization Type Materials Research and Development Project (grant no. JPMXP1121467561). Additionally, this work was supported by the National Institute for Materials Science (NIMS) Battery Research Platform.

Conflict of Interest

The authors declare no conflict of interest.

Keywords: experimental automation · high-throughput experiment · lithium-ion batteries · multicomponent electrolyte · solid electrolyte interfaces

[1] K. Xu, *Chem. Rev.* **2014**, *114*, 11503.
[2] E. Peled, S. Menkin, *J. Electrochem. Soc.* **2017**, *164*, A1703.
[3] A. Dave, J. Mitchell, K. Kandasamy, H. Wang, S. Burke, B. Paria, B. Póczos, J. Whitacre, V. Viswanathan, *Cell Rep. Phys. Sci.* **2020**, *1*, 100264.
[4] J. T. Yik, L. Zhang, J. Sjölund, X. Hou, P. H. Svensson, K. Edström, E. J. Berg, *Digital Discovery* **2023**, *2*, 799.
[5] A. Dave, J. Mitchell, S. Burke, H. Lin, J. Whitacre, V. Viswanathan, *Nat. Commun.* **2022**, *13*, 5454.
[6] J. Noh, H. A. Doan, H. Job, L. A. Robertson, L. Zhang, R. S. Assary, K. Mueller, V. Murugesan, Y. Liang, *Nat. Commun.* **2024**, *15*, 2757.
[7] A. Suzumura, H. Ohno, N. Kikkawa, K. Takechi, *J. Power Sources* **2022**, *541*, 231698.
[8] S. Matsuda, K. Nishioka, S. Nakanishi, *Sci. Rep.* **2019**, *9*, 6211.
[9] S. Matsuda, G. Lambard, K. Sodeyama, *Cell Rep. Phys. Sci.* **2022**, *3*, 100832.
[10] R. Tamura, K. Tsuda, S. Matsuda, *Adv. Mater. Methods* **2023**, *3*, 2232297.
[11] T. Taskovic, A. Eldesoky, C. P. Aiken, J. R. Dahn, *J. Electrochem. Soc.* **2022**, *169*, 100547.
[12] E. Logan, A. Eldesoky, E. Eastwood, H. Hebecker, C. Aiken, M. Metzger, J. Dahn, *J. Electrochem. Soc.* **2022**, *169*, 040560.
[13] T. Taskovic, A. Eldesoky, W. Song, M. Bauer, J. R. Dahn, *J. Electrochem. Soc.* **2022**, *169*, 40538.
[14] R. Fong, U. von Sacken, J. R. Dahn, *J. Electrochem. Soc.* **1990**, *137*, 2009.
[15] K. Xu, U. Lee, S. S. Zhang, T. R. Jow, *J. Electrochem. Soc.* **2004**, *151*, A2106.
[16] C. Täubert, M. Fleischhammer, M. Wohlfahrt-Mehrens, U. Wietelmann, T. Buhrmester, *J. Electrochem. Soc.* **2010**, *157*, A721.
[17] S. S. Zhang, K. Xu, T. R. Jow, *J. Electrochem. Soc.* **2002**, *149*, A586.

Manuscript received: December 10, 2024
Revised manuscript received: March 19, 2025
Version of record online: March 21, 2025